Publishing House
AKAPIT

COMPUTER METHODS IN MATERIALS SCIENCE

Informatyka w Technologii Materiałów

Vol. 11, 2011, No. 1

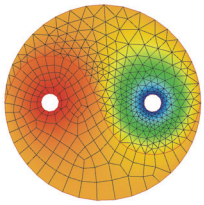

APPLICATION OF VISCOPLASTIC-DAMAGE MODELS TO QUASI-STATIC ICE FAILURE UNDER COMPRESSION

HYE-YEON CHOI, CHI-SEUNG LEE, BYUNG-MOON YOO, JAE-MYUNG LEE*

Department of Naval Architecture and Ocean Engineering, Pusan National University, Busan 609-735, Republic of Korea
**Corresponding author: jaemlee@pusan.ac.kr*

Abstract

In the present paper, the material behavior characteristics of fresh ice, such as material failure as well as constitutive behavior, have been evaluated based on the viscoplastic-damage mechanism. Ice is considered as one of the most complex materials in nature since it has various amounts and sizes of grain boundaries. The material behavior also significantly differs between the quasi-static and dynamic strain rates, namely, it has ductile and brittle material characteristics, respectively. In particular, the ice behavior under quasi-static strain rate is more complicated than under dynamic strain rate due to its ductile behavior, strain softening phenomenon, etc. Therefore, in the present paper, the unified viscoplastic model has been adopted to describe this phenomenon of ice under quasi-static strain rate. The material failure phenomenon of ice under compressive loading has been evaluated to avoid the fraction growth damage mechanism. The rate-dependent viscoplastic-damage model has been implicitly formulated and implemented to the ABAQUS user defined subroutine to simulate the ice failure quantitatively. In order to validate the proposed analysis method, the simulation results of ice failure have been compared to a series of compression tests of ice.

Key words: ice, unified viscoplastic-damage model, continuum damage mechanics, finite element analysis, failure, polar engineering

1. INTRODUCTION

There are many factors that affect the material nonlinearities of ice such as loads, strain rate, temperature, impurities contents, grain boundaries amount/size and crystalline orientation (Karr &Choi, 1989). Among these, the strain rate is one of the most effective factors. Similar to concrete and glass, ice is generally considered to be a brittle material. However, the viscoplastic response can be observed at low strain rate and melting point.

The mechanical behaviors of ice including brittle/ductile characteristics under arbitrary loads such as brittle fracture and creep have been carried out over several decades. In these studies, the elastic and/or viscoelastic material model has been adopted in order to conveniently adopt a numerical method such as the finite element method (Bhat & Xirouchakis, 1985). However, it seems impossible to apply these models to ductile ice behavior. Because the ice behavior under quasi-static strain rate represents the time-dependent material nonlinearities, it is essential to adopt the time-dependent viscoplastic constitutive model. In the present paper, the well-known Bodner-Partom (BP) form unified viscoplastic model has been adopted. The original BP model has been used to describe the creep behavior of metal under high temperature (Bodner, 2002), and various modifications have been performed by several groups of researchers in order to represent the various material behaviors of alloy metal, rubber, polymer, etc. Among these, one of the most robust

 ISSN 1641-8581

modified BP models has been chosen to describe the strain softening phenomenon of ice under quasi-static strain rate (Zairi et al., 2007).

The ice failure phenomenon is quite complex to calculate numerically because it is quite difficult to describe the material degradation quantitatively. As an alternative mechanism to solve this problem, the continuum damage mechanics have been spotlighted over several decades. The material degradation phenomenon can be calculated based on a damage variable which is a function of stress, inelastic strain tensor and other state variables. In the present paper, the Gurson-Tvergaard fraction growth model, which is one of the most popular damage models among others, has been adopted to capture the ice failure phenomenon specifically.

The unified viscoplastic-damage model has been formulated as a fully implicit formula and has been implemented to the ABAQUS user defined subroutine to predict the viscoplastic and damage behavior of ice under compressive loads. The proposed application technique based on FEA has been compared to a series of compression tests of ice to ensure validation.

2. EXPERIMENTS

A series of compression tests of ice under quasi-static strain rate has been carried out. Defects such as air inclusion and impurities have been removed during the freezing of the ice specimen. The horizontal, vertical and height dimensions of the ice specimen are 60 mm, 60 mm and 120 mm, respectively.

The compression test of ice has been performed in a universal test machine with a cryogenic chamber (left side of figure 1). In order to obtain the precise compressive stress-strain relationship, the stainless steel secondary jig and slip-prevention paper has been equipped at both edges of the ice specimen (right side of figure 1). The various strain rates have been adopted to recognize the rate-dependent viscoplastic characteristics of ice, namely, 0.7E-04S^{-1} to 2.8E-04S^{-1}. The ice test specimen has been pre-cooled at -10^{O}C before the compression test. In order to capture the ice failure procedure, the strain-controlled compressive loads have been removed at certain strains, i.e., 1%, 1.8%, 3% and 4% strains. The experimental void fraction was estimated quantitatively by drawing cross stripes upon capture and calculating the damaged area at each certain strain. The representative failure pattern of the ice specimen is shown in figure 2.

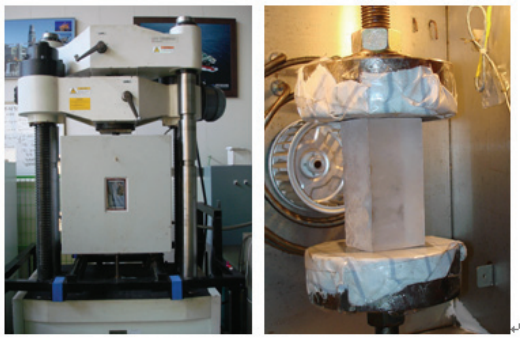

Fig. 1. *Experimental facilities for compression test of ice specimen.*

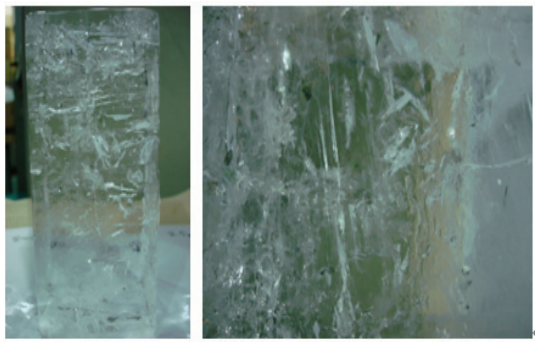

Fig. 2. *Photograph of representative ice failure at 1.8% strain.*

3. THEORIES

3.1. Unified Viscoplastic Constitutive Model

In order to describe the strain softening phenomenon of ice, the modified BP model has been adopted (Zairi et al., 2005; Zairi et al., 2007).
Neglecting temperature effects, the total elastic rate can be decomposed as,

$$\dot{\varepsilon}_{ij} = \dot{\varepsilon}^{e}_{ij} + \dot{\varepsilon}^{p}_{ij} \tag{1}$$

where $\dot{\varepsilon}_{ij}$ is the total strain rate tensor, $\dot{\varepsilon}^{e}_{ij}$ is the elastic strain rate tensor and $\dot{\varepsilon}^{p}_{ij}$ is the plastic strain rate tensor.
The elastic components are provided by the time derivative of the generalized Hooke's law

$$\dot{\sigma}_{ij} = D_{ijkl}\dot{\varepsilon}^{e}_{kl} \tag{2}$$

where
$D_{ijkl}\left(=2G\left[(1/2)\left(\delta_{ik}\delta_{jl}+\delta_{il}\delta_{jk}\right)+\left(\nu/1\text{-}2\nu\right)\delta_{ij}\delta_{kl}\right]\right)$ is the elastic stiffness tensor, G is the shear modulus, ν is the Poisson's ratio and δ_{ij} is the Kronecker delta function.

The viscoplastic strain components are represented by the isotropic form of the Prandtl-Reuss flow law,

$$\dot{\varepsilon}_{ij}^{p} = \lambda S_{ij} \tag{3}$$

where λ is the plastic multiplier and $S_{ij}\left(=\sigma_{ij}-(1/3)\sigma_{kk}\delta_{ij}\right)$ is the deviatoric stress tensor.

The plastic multiplier representing hardening can be defined as,

$$\lambda = \frac{D_0}{\sqrt{J_2}}\left(\frac{3J_2}{Z^2}\right)^n \tag{4}$$

where D_0 is the limiting shear-strain rate, n is the strain rate sensitivity parameter, Z is the total hardening variable and J_2 is the second deviatoric invariant.

The evolution laws can be derived as follows: The state variable Z can be decomposed into components representing isotropic hardening and kinematic hardening.

In the present paper, the kinematic hardening is not considered in order to represent the strain softening effects. The isotropic hardening Z^{I} can be decomposed into the hardening part Z_1^{I} and softening part Z_2^{I} respectively,

$$Z^{\mathrm{I}} = Z_1^{\mathrm{I}} + Z_2^{\mathrm{I}} \tag{5}$$

The components $\dot{Z}_1^{\mathrm{I}}$ and $\dot{Z}_2^{\mathrm{I}}$ can be defined as,

$$\dot{Z}_1^{\mathrm{I}} = \lambda m\left[\frac{Z_1^{\mathrm{I}} - (1-\alpha)Z_{10}}{Z_{10}}\right]S_{kl}S_{kl} \tag{6}$$

$$\dot{Z}_2^{\mathrm{I}} = \lambda h\left(1-\frac{Z_2^{\mathrm{I}}}{Z_{2s}}\right)S_{kl}S_{kl} \tag{7}$$

where Z_{10} is the initial value of Z_1, m is the rate parameter of hardening, α is the hardening parameter controlling the resumption of the strain hardening, h is the rate parameter of softening and Z_{2s} is the saturation value of Z_2. The material parameters of the modified BP model, $\alpha = 0.02$, $Z_{10} = 363$, $Z_{2s} = -30$, $n = 2.10$, $m = 900$ and $h = -10$ were found at the loading rate of 1mm/min (Zairi et al., 2007) and the elastic modulus of ice was defined as $E = 700$ MPa which is the mean value of all elastic moduli of the compressive tests.

3.2. Damage Model

The concept of a continuum damage model was first introduced by Kachanov (1958) to describe the effects of an isotropic distribution of spherical voids on plastic flow. In this approach, a state variable which is termed 'damage' is introduced to describe the material degradation due to the presence of voids. One of the most popular damage models to calculate the void fraction of materials, the Gurson-Tvergaard fraction growth model (Gurson, 1977; Tvergaard, 1981), has been introduced as,

$$\Phi(\sigma_{ij},\sigma_0,f) = \left(\frac{\sigma_e}{\sigma_0}\right)^2 + 2fq_1\cosh\left(\frac{3}{2}q_2\frac{\sigma_h}{\sigma_0}\right) - 1 - q_3f^2 = 0 \tag{8}$$

where Φ is the Gurson–Tvergaard's flow potential, σ_0 is the yield stress, σ_e is the Mises effective stress, σ_h is the macroscopic hydrostatic stress, f is the current void volume fraction and q_1, q_2, q_3 parameters introduced by Tvergaard (1981).

The void volume fraction rate $\dot{f}$ can be decomposed into the void growth part $\dot{f}_{grow}$ and the void nucleation part $\dot{f}_{nuc}$ as follows,

$$\dot{f} = \dot{f}_{grow} + \dot{f}_{nuc} \tag{9}$$

The void growth rate is given by the mass conservation principle, namely,

$$\dot{f}_{grow} = (1-f)\mathrm{tr}(D_{ij}^{P}) \tag{10}$$

where the trace of viscoplastic strain rate, $\mathrm{tr}(D_{ij}^{P})$ is given by,

$$\mathrm{tr}(D_{ij}^{P}) = 3\Lambda q_1q_2\frac{f}{\sigma_e}\sinh\left(\frac{3}{2}q_2\frac{\sigma_h}{\sigma_e}\right) \tag{11}$$

The first term of the upper equations is given by,

$$\Lambda = (1-f)\sigma_e\dot{p}\left(\Sigma_{ij}:\frac{\partial\Phi}{\partial\Sigma_{ij}}\right)^{-1} \tag{12}$$

where $\sum_{ij}$ is the stress tensor and $\dot{p}$ is the plastic strain rate $\dot{\varepsilon}^{p}$.

To capture the accelerated damage due to cavitation of voids, according to the phenomenological

hydrostatic stress controlled nucleation law proposed by Jeong (2001), the nucleation part can be given by,

$$\dot{f}_{nuc} = \frac{f_N}{sZ_{10}\sqrt{2\pi}} \exp\left[-\frac{1}{2}\left(\frac{\sigma_h - \sigma_N}{sZ_{10}}\right)^2\right]\dot{\sigma}_h \quad (13)$$

Where s is the standard deviation, σ_N is the mean value of the hydrostatic stress and f_N is the volume fraction of ice particles. We found the material parameters of the Gurson – Tverggard fraction growth model, which are $q_1 = 5$, $q_2 = 5$, $q_3 = 5$, s = 0.1, $\sigma_N = 1$, $f_N = 0.99$ (Zairi et al., 2005).

4. IMPLICIT FORMULATION AND COMPUTATIONAL ALGORITHM

4.1. Implicit Formulation for application to ABAQUS user defined subroutine

The aforementioned viscoplastic-damage model has been implicitly formulated in order to computationally calculate the ice material behavior using ABAQUS. One of the ABAQUS user defined subroutines, UMAT, provides the information of the state variables such as strain, stress, etc. related to each incremental step. All of the state variables have been updated during calculations. The optimal size of the analysis time increment Δt and the corresponding strain increment are determined using the material Jacobian matrix. The numerical integration scheme which is used in the present paper is described as follows (Anderson, 2003).

The incremental strain is given by,

$$\varepsilon_{ij}^{n+1} = \varepsilon_{ij}^{n} + \Delta\varepsilon_{ij} \quad (14)$$

The corresponding elastic trial stress tensor is computed from,

$$\hat{\sigma}_{ij}^{n+1} = \sigma_{ij}^{n} + D_{ijkl}\Delta\varepsilon_{ij} \quad (15)$$

where $\hat{\sigma}_{ij}$ is the trial stress tensor.

The stress updates can be written as,

$$\sigma_{ij}^{n+1} = \hat{\sigma}_{ij}^{n+1} - \Delta\lambda D_{ijkl} S_{ij}^{n+1} \quad (16)$$

The scalar $\Delta\lambda$ according to the definition $\lambda\Delta t$ can be written with damage,

$$\Delta\lambda = \frac{D_0}{\sqrt{J_2}}\left\{\frac{3J_2}{[Z(1-f)]^2}\right\}^n \Delta t \quad (17)$$

At the end of the increment, the time history values for every solution dependent state variable are stored. The following equations are representative state variables for the constitutive equations

$$Z^{n+1} = Z_1^{n+1} + Z_2^{n+1} \quad (18)$$

$$Z_1^{n+1} = Z_1^{n} + \Delta m\left[\frac{Z_1^I - (1-\alpha)Z_{10}}{Z_{10}}\right]2J_2 \quad (19)$$

$$Z_2^{n+1} = Z_2^{n} + \Delta\lambda h\left(1 - \frac{Z_2^I}{Z_{2s}}\right)2J_2 \quad (20)$$

$$f_{grow}^{n+1} = f_{grow}^{n} + (1-f)\mathrm{tr}(D_{ij}^P)\Delta t \quad (21)$$

$$f_{nuc}^{n+1} = f_{nuc}^{n} + \frac{f_N}{sZ_{10}\sqrt{2\pi}} \exp\left[-\frac{1}{2}\left(\frac{\sigma_h - \sigma_N}{sZ_{10}}\right)^2\right]\dot{\sigma}_h\Delta t \quad (22)$$

The Newton-Raphson method is adopted in ABAQUS solver. Hence, it is essential to calculate the material Jacobian matrix, $\partial\Delta\sigma_{ij} / \partial\Delta\varepsilon_{kl}$ as follows,

$$\frac{\partial\Delta\sigma_{ij}}{\partial\Delta\varepsilon_{kl}} = D_{ijkl} = D_{ijkl}^a - \frac{1}{\Omega} D_{ijmn}^a S_{mn} \Psi_{op} D_{opkl}^a \quad (23)$$

4.2. Computational Algorithm

Figure 3 shows the computational algorithm of the present paper. The numerical analysis is carried out in ABAQUS/Standard platform and the material nonlinear analysis is performed by the developed UMAT. In order to simulate the material failure of ice, the element weakening method is adopted (Mishnaevsky, 2005). In other words, based on the calculated damage variables, the damage related material properties such as stiffness, hardening, softening, etc. of each element are modified and material degradation is performed.

5. NUMERICAL EXAMPLES

5.1. Finite Element Model for Ice

In order to verify the developed computational analysis technique, the analysis results have been compared to a series of compression tests of ice. Figure 4 shows the finite element model and boundary condition for the ice test specimen of the compression test. An 8-node hexahedron element (C3D8R element in ABAQUS) is adopted. The total

number of elements and nodes are 3456 and 4225, respectively.

Fig. 3. *Computational algorithm using ABAQUS user defined subroutine UMAT.*

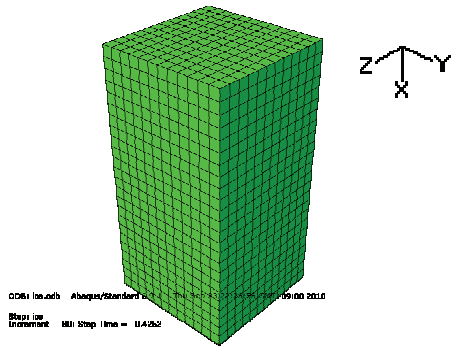

TOP - X, Y, Z (FIXED)
BOTTOM - X (STRAIN CONTROLLED) Y, Z (FIXED)

Fig. 4. Finite element model for ice test specimen of compression test.

5.2. Prediction of Viscoplastic Behavior of Ice

Figures 5 and 6 show the stress-strain relationship between experiments and simulation results regarding the 1.4E-04 and 2.8E-04 strain rates, respectively. As shown in these graphs, the strain softening phenomenon of ice under quasi-static compressive loads has been observed. Moreover, the typical characteristics of viscoplastic material behavior, i.e., increase of yield/tensile strength and ductility, have been captured. These phenomena have been precisely predicted using the proposed computational analysis technique.

5.3. Prediction of Material Failure of Ice

Figure 7 shows the quantitive damage comparison between experiments and simulations at 1.8%, 3% and 4% strains when the strain rate is cimen of compression test a 1 mm/min displacement rate (1.4E-04 strain rate). As shown in figure 7, the ice failure is concentrated on the region of the top surface (x, y and z fixed surfaces) at 1.8% strain due to the effect of the reaction force. The void fraction then grows quite rapidly through all of the directions at 3% strain. At 4% strain, the ice specimen has totally failed and collapsed.

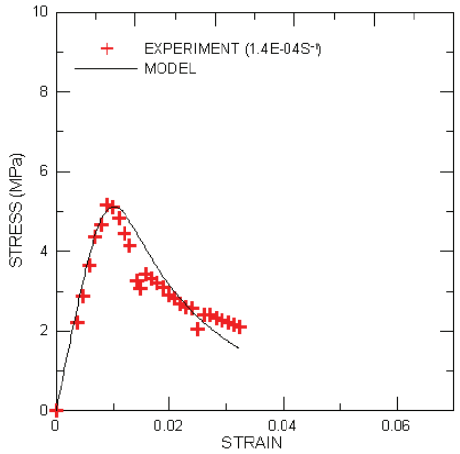

Fig. 5. *Stress-strain relationship between experiments and simulation at 1.4E-04 strain rate.*

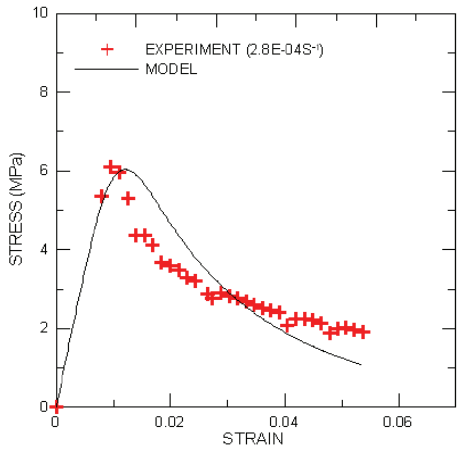

Fig. 6. *Stress-strain relationship between experiments and simulation at 2.8E-04 strain rate.*

These phenomena have also been qualitatively simulated using the proposed computational analysis technique. Although the specific crack pattern could not be predicted, the void fraction contour has been successfully described (figure 8).

In order to calculate the amount of void fraction quantitatively, the experimental void fraction was estimated by drawing cross stripes upon capture and

calculating the damaged area; the void fraction volume of simulation has also been estimated by calculating damaged elements. The damaged area was divided into all areas to calculate the fraction factor. Table 1 shows the comparison of void fraction volume between experiments and simulations, and the computational analysis results coincide well with the experimental results.

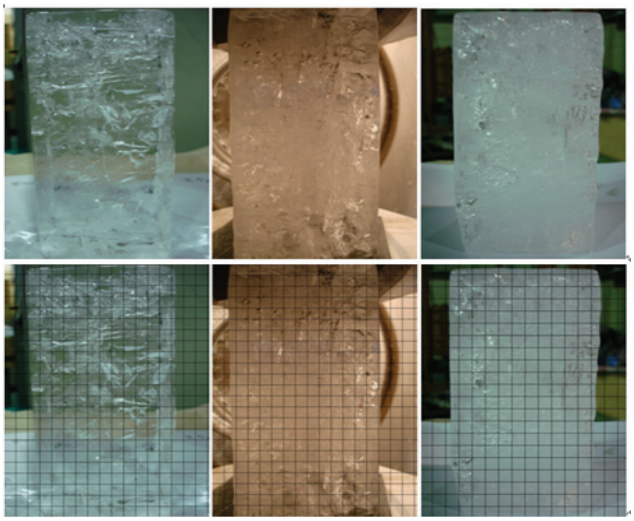

Fig. 7. *Quantitive damage comparison between experiments and simulations (left: 1.8%, middle: 3%, right: 4% strain).*

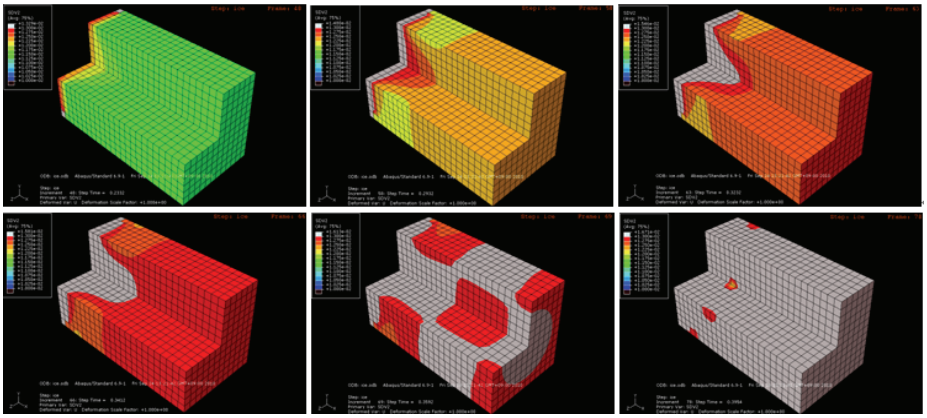

Fig. 8. *Void fraction contour.*

Table 1. *Fraction factor.*

Strain	Experiments	Simulations	Error (%)
1.8%	0.39	0.43	4
3.0%	0.89	0.90	1
4.0%	0.98	0.99	1

6. CONCLUDING REMARKS

A useful computational algorithm based on a user subroutine has been developed to predict the behavior of ice as well as the results of a compressive test. The ABAQUS user defined subroutine UMAT for ice has been developed based on the rate dependent unified viscoplastic constitutive model (Bodner, 2002), coupled with the void fraction damage model (Gurson, 1977). We have adopted the void fraction damage model to describe the fracture of ice since the direction of crack propagation on ice is complicated and void nucleation and void growth affect damage simultaneously. The viscoplastic damage model has been verified by comparing the results of the compressive test and computational results, and a void fraction contour has also been simulated successfully. The quantitive damage comparisons between experiments and simulations were in good agreement.

It is our hope that the developed computational algorithm can help to estimate ice load fundamentally, and to give useful information to develop suitable computational methodology for ice.

ACKNOWLEDGEMENTS

This paper is part of “A Development of the Safe Operation Methodology of Ice-class Vessel at Arctic Sea Route and the Cryogenic Evaluation Techniques for the Ice Performance - Part 1: Safety Assessment Techniques for Hull Structure of Icebreaking Vessels" supported by the Ministry of Knowledge and Economy, Korea. Financial support through the Industrial Strategic Technology Development Program (Grant No. 10033640) is greatly acknowledged.

REFERENCES

Anderson, H., 2003, An Implicit Formulation of the Bonder-Partom Constitutive Equations, *Comp. Struc.*, 81, 1405-1414.

Bhat, S.U., Xirouchakis, P.C., 1985, Rigid-Plastic Analysis of Floating Plates, *J. Eng. Mech.*, 111, 815-831.

Bodner, S.R., 2002, *Unified Plasticity for Engineering Applications*, Kluwer Academic & Plenum Publishers, New York.

Gurson, A.L., 1977, Continuum Theory of Ductile Rupture by Void Nucleation and Growth, *J. Eng. Mat. Tech.*, 99, 2-15.

Jeong, H.Y., Pan, J., 1995, A Macroscopic Constitutive Law for Porous Solid with Pressure Sensitive Matrices and Its Implications to Plastic Flow Localization, *Int. J. Sol. Struc.*, 32, 1385-1403.

Kachanov, L.M., 1958, On the Time to Failure Under Creep Conditions, *IZV Akademie Naukovi SSSR O.T.N. Tekhika Naukovi*, 8, 26-31.

Karr, D.G., Choi, K., 1989, A Three-dimensional Constitutive Damage Model for Polycrystalline Ice, *Mech. Mat.*, 8, 55-66.

Mishnaevsky, L. Jr., 2007, *Computational Mesomechanics of Composites*, John Wiley & Sons, Inc., Chichester.

Tvergaard, V., 1981, Influence of Voids on Shear Band Instabilities under Plane Strain Conditions, *Int. J. Frac.*, 17, 389-407.

Zairi, F., Abdelaziz, M.N., Woznica, K., Gloaguen, J.M., 2005, Constitutive Equations for the Viscoplastic-Damage Behavior of a Rubber-Modified Polymer, *Euro. J. Mech. A.*, 24, 169-182.

Zairi, F., Abdelaziz, M.N., Woznica, K., Gloaguen, J.M., 2007, Elasto-viscoplastic Constitutive Equations for the Description of Glassy Polymers Behavior at Constant Strain Rate, *J. Eng. Mat. Tech.*, 129, 29-35.

ZASTOSOWANIE LEPKOPLASTYCZNYCH MODELI ZNISZCZENIA DO OPISU QUASI-STATYCZNEGO PĘKANIA LODU W WARUNKACH ŚCISKANIA

Streszczenie

W pracy dokonano oceny zachowania się świeżego lodu w aspekcie jego pękania oraz parametrów konstytutywnych. Zastosowano lepkoplastyczny model zniszczenia. Lód jest uważany za jeden z bardziej skomplikowanych materiałów w naturze, ponieważ ma on różną liczbę i długość granic ziaren. Zachowanie się tego materiału różni się znacząco pomiędzy quasi-statycznymi i dynamicznymi prędkościami odkształcenia, to znaczy lód ma w tych stanach odpowiednio plastyczną i kruchą charakterystykę. Zachowanie się lodu w warunkach quasi-statycznych jest znacznie bardziej skomplikowane niż przy obciążeniach dynamicznych, co jest spowodowane występowaniem kruchości a także mięknięciem pod wpływem odkształcenia. W niniejszej pracy przystosowano lepkoplastyczny model do opisu zjawisk zachodzących w lodzie w warunkach quasi-statycznych. Oceniono zjawisko zniszczenia lodu pod wpływem obciążeń ściskających tak aby uniknąć wywołania mechanizmu wzrostu pęknięcia. Zależny od prędkości lepkoplastyczny model pękania został sformułowany i zaimplementowany w programie ABAQUS jako procedura użytkownika. Pozwoliło to na ilościowe przewidywanie pękania lodu. W celu weryfikacji zaproponowanej metody wyniki symulacji pękania lodu porównano z wynikami prób ściskania.

Received: September 30, 2010
Received in a revised form: November 2, 2010
Accepted: November 25, 2010